Flexural Strengthening of Prestressed Bridge Slabs with FRP Systems

Tarek Hassan
Ph.D. Candidate
Department of Civil and
Geological Engineering
University of Manitoba
Winnipeg, Manitoba, Canada

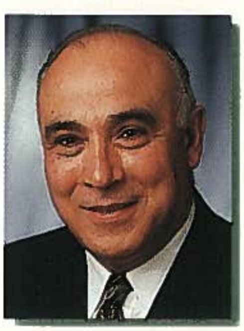

Sami Rizkalla, Ph.D., P.E.
Distinguished Professor
Department of Civil Engineering
North Carolina State University
Raleigh, North Carolina

Fiber reinforced polymer (FRP) materials offer great potential for cost-effective retrofitting of concrete structures. In response to the growing need for strengthening and rehabilitation of concrete structures and bridges, an experimental program was conducted to investigate the feasibility of using different strengthening techniques as well as different types of FRP for strengthening prestressed concrete members. Half-scale models of a prestressed concrete bridge were constructed and tested to failure. The test specimens consisted of one simple span and two overhanging cantilevers. Each specimen was tested three times using a different load location in each case. Five different strengthening techniques were investigated including near surface mounted Leadline bars, C-Bars, CFRP strips and externally bonded CFRP sheets and strips. Ultimate capacity, failure mechanism and cost analysis of various strengthening techniques for concrete bridges are presented. The applicability of a nonlinear finite element analysis of post-tensioned bridge slabs strengthened with near surface mounted FRP reinforcement is enumerated.

In an aggressive environment, concrete may be vulnerable to chemical attacks such as carbonation and chloride contamination which breaks down the alkaline barrier in the cement matrix. Consequently, the steel reinforcement in concrete structures becomes susceptible to rusting and corrosion. Such a phenomenon leads to delamination of the concrete at the reinforcement level, cracking and spalling of the concrete under more severe conditions.

In the United States, nearly one-third of the nation's 581,000 bridges were found to be structurally deficient or functionally obsolete.[1] A large number of these deficient bridges are reinforced or prestressed concrete structures, and are in urgent need of repair and strengthening. In the United Kingdom, over 10,000 concrete bridges need structural attention. In Europe, it is estimated that the repair of structures due to corrosion of reinforcing bars in reinforced concrete structures

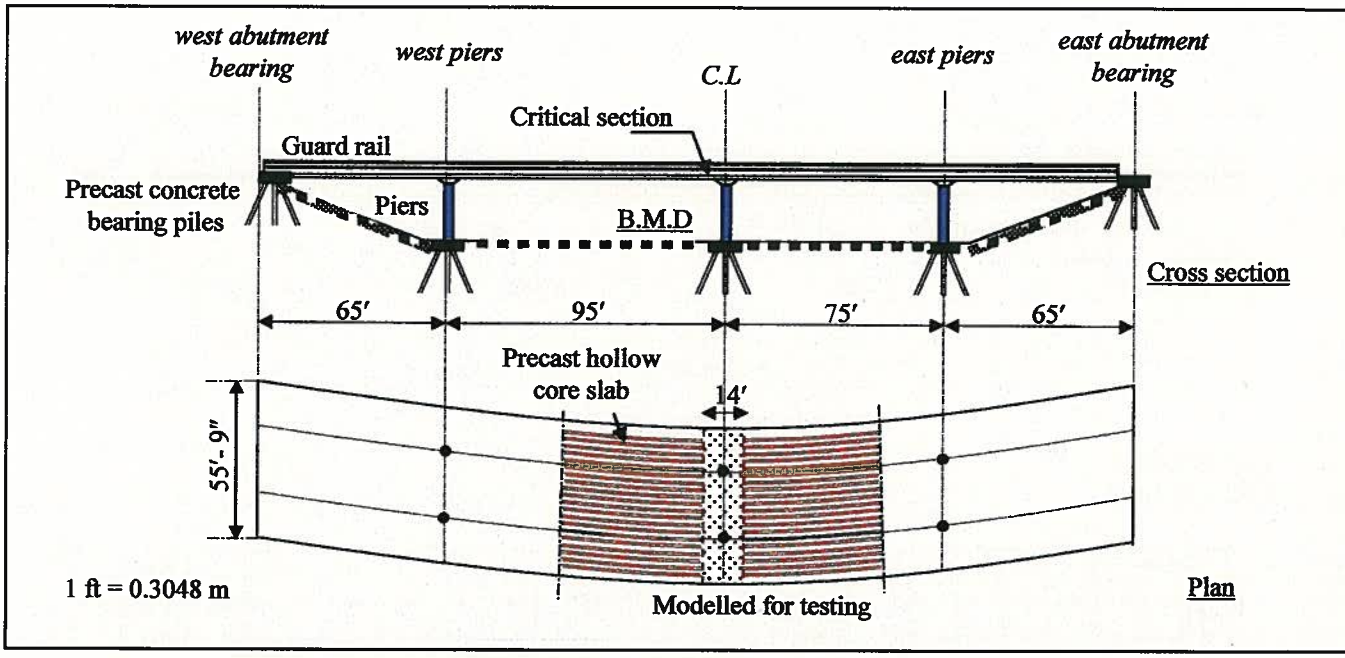

Fig. 1. Schematic of Bridge No. 444 in Winnipeg, Manitoba, Canada.

costs over $600 million annually.[2]

A possible solution to combat reinforcement corrosion for new construction is the use of non-corrosive materials to replace conventional steel bars. High tensile strength, lightweight and corrosion resistance characteristics make FRP (fiber reinforced polymer) ideal for such applications. FRP also provides a cost effective and practical technique for the repair and strengthening of structures and bridges using externally bonded sheets or prefabricated laminates. FRP tendons can also be used to strengthen old prestressed concrete girders as well as to prevent corrosion in tendons from occurring in salty regions.[3,4]

The needs to study the most appropriate strengthening technique for prestressed concrete bridges are initiated by the necessity to upgrade a 30-year-old concrete bridge in Winnipeg, Manitoba, Canada. A bridge rating analysis conducted using the current AASHTO (American Association of State Highway and Transportation Officials) Specifications indicated that the flexural strength of the bridge deck is not sufficient to withstand modern truck loads.[3] To accommodate the AASHTO HSS30 truck design load, the analysis indicated a need to increase the flexural strength by approximately 10 percent at the negative moment zone over the pier columns where the maximum shear is located.

Bridge replacement costs were estimated to exceed $1.6 million (USD). Therefore, it was decided to consider strengthening the bridge using FRP. Site inspections indicated extensive transverse and longitudinal cracking of the top surface of the bridge deck. The underside of the deck was generally in good condition. Based on site inspections, the bridge does not need to be demolished and replaced. It can be feasibly and economically rehabilitated.

Due to the lack of information on the use of near surface mounted FRP reinforcement for flexural strengthening in regions of combined bending and high shear stresses, the reported experimental program in this paper has been undertaken. Three half-scale models of the bridge under consideration were cast and post-tensioned. The specimens were tested in simple span with a double cantilever configuration. Each specimen was tested three times using loads applied at different locations in each test.

The first and second tests were performed on the two cantilevers where the load was applied at the edge of each cantilever. The third test was conducted using a load applied at midspan. Prior to the midspan test, the cracks resulting from testing the two cantilevers were sealed completely by injecting them with a high strength epoxy resin adhesive. The midspan section was then strengthened using FRP reinforcement and tested.

RESEARCH SIGNIFICANCE

This paper demonstrates the cost effectiveness of five different strengthening techniques using FRP for flexural strengthening of post-tensioned concrete bridge slabs. The significance of this project is that the flexural strengthening is located at the zones of maximum shear stresses typically occurring at the maximum negative moment section of cantilevers and continuous beams. The research provides experimental evidence and detailed performance of various FRP strengthening techniques.

The paper also provides a cost analysis for each technique to help engineers to select the most appropriate system for flexural repair and strengthening of concrete structures and bridges. The development of cost-effective and durable restorative systems will extend the service life of deteriorated civil infrastructures and ensure safety of the public.

TEST SPECIMENS

The test specimens simulate the post-tensioned solid slab over the in-

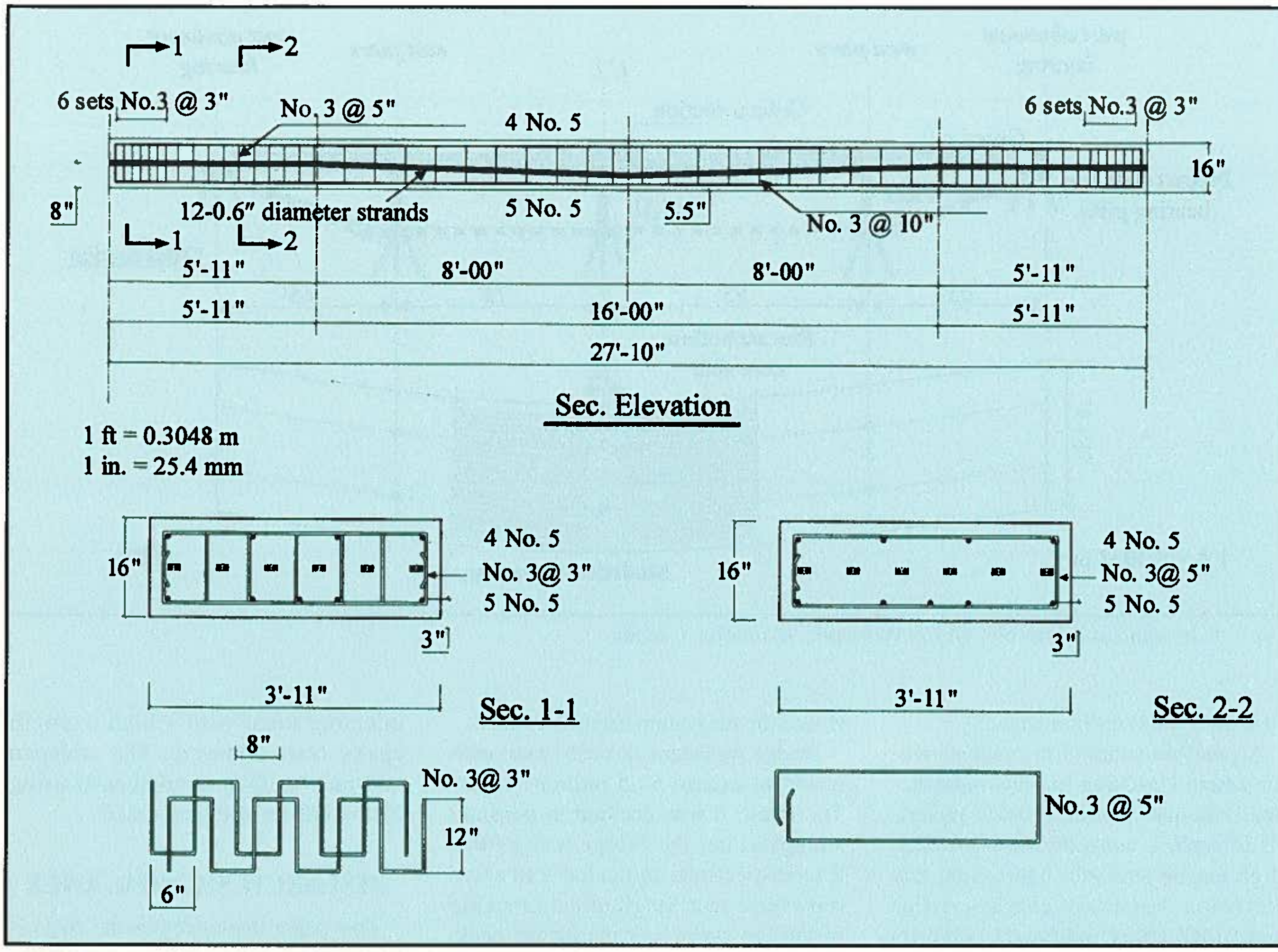

Fig. 2. Reinforcement details of test specimens.

termediate pier columns of a bridge constructed in the early 1970s in Winnipeg, Manitoba, Canada. The bridge consists of four spans, as shown in Fig. 1, and was designed for AASHTO HSS20 truck design loading.[5] The thickness of the bridge slab along the spans is 32 in. (810 mm), cast in place, partially voided and post-tensioned. The solid slab over the intermediate pier columns is post-tensioned transversely to resist the negative moments at the columns and the positive moment at midspan.

To simulate the combined effect of high flexural and shear stresses at the intermediate supports of the bridge, three half-scale models of the solid slab designated as S1, S2, and S3 were constructed. The support configuration of the specimens was designed to examine the FRP repair system at the zones of maximum negative moment at the support, which coincides with the maximum shear.

The number and layout of the tendons were selected to have the same stress level of the bridge under service load conditions. The critical bending moments for the bridge were evaluated based on a linear elastic finite element analysis using a commercial computer program, SAP2000.[6] The loss of the prestressing force was calculated according to the current AASHTO Specifications.[5]

The specimens were reinforced with four No. 5 mild steel bars on the top surface and five No. 5 mild steel bars on the bottom surface. The bars have a yield strength of 60 ksi (400 MPa) and an elastic modulus of 29,000 ksi (200 GPa). The number of bars in the top surface was selected to represent the same reinforcement ratio in the cantilever portion of the bridge.

Shear reinforcement consisted of No. 3 U-shaped stirrups. The stirrups were spaced at 5 in. (127 mm) on center in the cantilever span and 10 in. (254 mm) on center in the simply supported span. Reinforcement details of the specimens are shown in Fig. 2.

Bursting reinforcement was provided using six pairs of No. 3 looped bars spaced at 3 in. (75 mm) on center. Twelve 0.6 in. (15 mm) seven-wire strands were used for post-tensioning the specimens. The compressive strength of concrete after 28 days ranged from 6500 to 7200 psi (45 to 50 MPa) for the three slabs.

STRENGTHENING TECHNIQUES

Slab S1

One cantilever of Slab S1 was strengthened using near surface mounted Leadline CFRP bars while the other cantilever remained unstrengthened. The Leadline bars were produced by Mitsubishi Chemicals Corporation, Japan. The bars have a modulus of elasticity of 21,000 ksi (147 GPa) and an ultimate tensile strength of 285 ksi (1970 MPa) as reported by the manufacturer. Based on equilibrium and compatibility conditions, six $^3/_8$ in. (10 mm) diameter Leadline CFRP bars were used to achieve a 30 percent increase in the ultimate load carrying capacity of the slab.

To strengthen the cantilever slab using near surface mounted bars, grooves had to be cut on the top surface of the concrete. The location of the grooves was first marked using a chalk line. The grooves were 8 in. (200 mm) apart. A concrete saw was used to cut six grooves approximately 0.6 in. wide and 1.2 in. deep (16 x 30 mm) at the tension surface of the cantilever as shown in Fig. 3.

Fig. 3. Cutting grooves for near surface mounted CFRP bars.

The groove ends were widened to provide wedge action and to prevent possible slippage of the bars. Tapering the ends of the grooves was intended to induce inclined frictional forces at the concrete-epoxy interface. These inclined forces provided radial confining forces on the bars and, consequently, increased the pullout resistance.

Kemko 040 epoxy adhesive was used for bonding the CFRP bars to the surrounding concrete. The epoxy was produced by ChemCo Systems, Inc., United States. The adhesive is commonly used for grouting bolts, dowels, and steel bars in concrete. The epoxy was pressure injected into the grooves to cover two-thirds of the groove height. The bars were placed in the grooves and gently pressed to displace the bonding agent as shown in Fig. 4. The grooves were then filled completely with the epoxy. Quality control was achieved through continuous inspections and measurements during the installation procedures.

After completion of the first two tests on both cantilevers, the resulting cracks were injected with epoxy. Based on an equilibrium and compatibility approach, ten $^3/_8$ in. (10 mm) diameter Leadline CFRP bars were used to achieve a 30 percent increase in the ultimate capacity of the midspan section of the simply supported slab. The grooves on the bottom surface were 4.7 in. (120 mm) apart. The same procedures as described before for cutting the grooves and placing the bars were applied.

Slab S2

The second slab, S2, was used to investigate the performance of both near surface mounted and externally bonded CFRP strips in strengthening of concrete bridges. Recently, test results of near surface mounted CFRP strips reported good and uniform bond distribution of the strips to the concrete and full utilization of the strength of the strip up to rupture.[7] The analysis indicated a need of six CFRP strips, 2 in. wide and 0.055 in. thick (50 x 1.4 mm), to achieve a 30 percent increase in the ultimate capacity of the cantilever slab.

The first cantilever was strengthened using six externally bonded CFRP strips. The concrete substrate was prepared by grinding the surface at the locations of the strips. The

Fig. 4. CFRP bars inserted in epoxy.

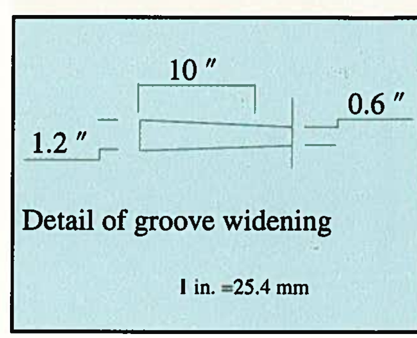

Fig. 5. Bonding CFRP strips to surface.

epoxy was then placed over the strips and on the concrete surface. Finally, the strips were placed on the concrete surface and gently pressed into the epoxy using a ribbed roller as shown in Fig. 5.

The second cantilever was strengthened also using six CFRP strips inserted into grooves cut at the top surface of the concrete. In order to insert the strips within the concrete cover layer, the strips were cut into two halves, each 1 in. (25 mm) wide. Using a concrete saw, grooves approximately 0.2 in. wide and 1 in. deep (5 x 25 mm) were cut at the tension surface of the second cantilever.

The grooves were injected with the epoxy adhesive to provide the necessary bond with the surrounding concrete as shown in Fig. 6a. The strips were then placed in the grooves and completely covered with the epoxy as shown in Fig. 6b.

The CFRP strips were produced by S&P Clever Reinforcement Company, Switzerland. The strips had a modulus of elasticity of 21,800 ksi (150 GPa) and an ultimate tensile strength of 290 ksi (2000 MPa) as reported by the manufacturer.

After testing both cantilevers, the areas above the supports were substantially cracked. To enable further testing of the midspan, the cracks were injected similar to Slab S1. Eighteen near surface mounted CFRP strips, 1 in. wide and 0.055 in. thick (25 x 1.4 mm), spaced by 2.6 in. (66 mm) on center were used to achieve a 30 percent increase in the ultimate capacity of the simply supported slab. En-Force CFL was used in bonding both near surface mounted and externally bonded CFRP strips to the concrete. The epoxy was produced by Structural Composites, Inc., United States.

Slab S3

A widespread method for the rehabilitation of concrete structures is the externally bonded CFRP sheets. This method can be seen as a state-of-the-art technique despite some detailing problems and design aspects that could influence the failure modes.

To investigate the effectiveness of this strengthening method in comparison to the three previously prescribed techniques, the simply supported span and one cantilever of Slab S3 were both strengthened using externally bonded CFRP sheets. The sheets were manufactured by Master Builders Technologies, Ltd., Ohio. The required area of CFRP sheets was calculated to achieve a 30 percent increase in the flexural capacity of the cantilever slab.

For the first cantilever, the sheets were applied in two plies. The first ply

Fig. 6a. Filling grooves with epoxy.

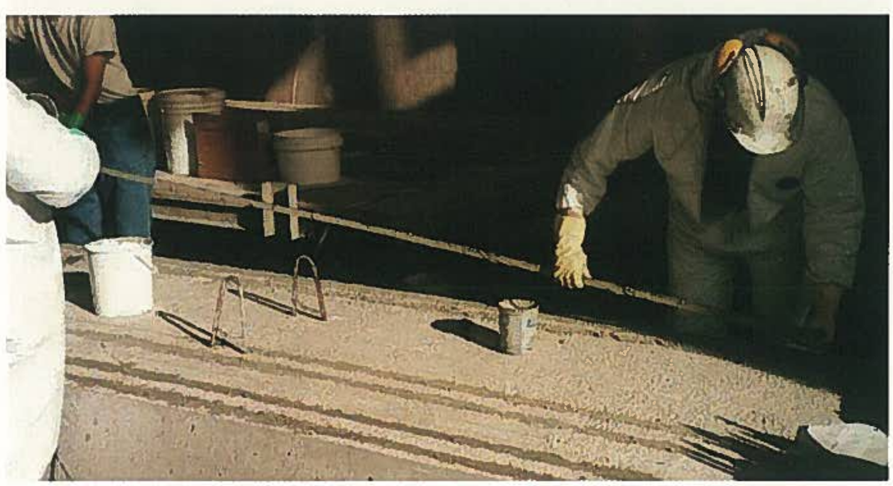

Fig. 6b. Inserting CFRP strips inside grooves.

covered the entire width of the slab while the second ply covered 19 in. (480 mm) and was centered along the width of the slab. Installation procedures are illustrated in Fig. 7. The sheets had a modulus of elasticity of 33,000 ksi (228 GPa) and an ultimate tensile strength of 620 ksi (4275 MPa) as reported by the manufacturer.

The second cantilever was strengthened using eight near surface mounted C-BAR CFRP bars. The bars were manufactured by Marshall Industries Composites Inc., United States. Based on testing, the bars had a modulus of elasticity of 16,100 ksi (111 GPa) and an ultimate tensile strength of 280 ksi (1918 MPa). The bars were sandblasted to enhance their bond to the epoxy adhesive. The bars were then inserted inside grooves cut at the top surface of the concrete. The grooves were 6 in. (150 mm) apart. The groove dimensions were 0.6 in. wide and 1.2 in. deep (16 x 30 mm).

The simply supported span was strengthened with externally bonded CFRP sheets after injecting the cracks resulting from cantilever tests. Three plies of CFRP sheets were used to achieve a 30 percent increase in flexural capacity. The first two plies covered the entire width of the slab, while the third ply covered 16 in. (400 mm) and was centered along the width of the slab. Detailed information about the tested specimens is provided in Table 1. The designation of the tested specimens are C or SS for cantilever or simply supported specimens, respectively.

TESTING SCHEME

The slabs were tested under static loading conditions using a uniform line-load acting on a width equivalent to the width of a tire contact patch according to the AASHTO HSS30 design vehicle. A closed-loop MTS 1200 kip (5000 kN) testing machine was used to apply the load using stroke control mode with a rate of 0.02 in./min (0.5 mm/min) up to failure.

Neoprene pads were placed between the steel beam and the slab to simulate the contact surface of a truck tire and to avoid local crushing of the concrete. For the cantilever tests, the load was

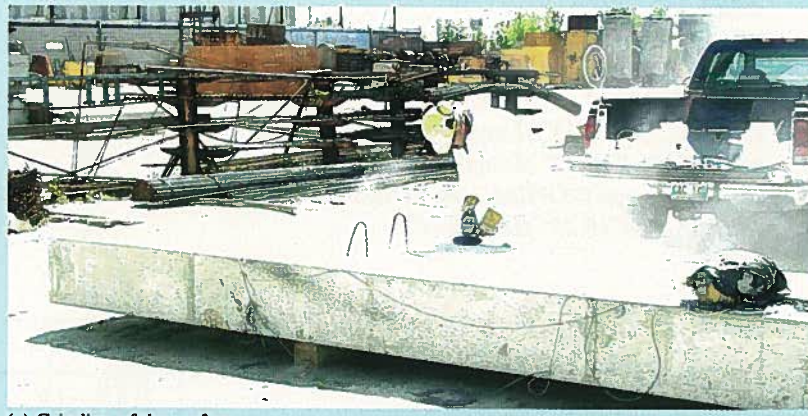

(a) Grinding of the surface

(b) Applying the MBrace saturant

(c) Bonding the CFRP sheets

Fig. 7. Installation procedures for externally bonded CFRP sheets.

Table 1. Details of test specimens.

Slab No.	Specimen	Strengthening technique
1	C1	Control specimen
	C2	6 No. 3 near surface mounted Leadline bars
	SS1	10 No. 3 near surface mounted Leadline bars
2	C3	6 Externally bonded CFRP strips (2 x 0.055 in.)
	C4	12 near surface mounted CFRP strips (1 x 0.055 in.)
	SS2	18 near surface mounted CFRP strips (1 x 0.055 in.)
3	C5	2 plies of externally bonded CFRP sheets
	C6	8 No.3 near surface mounted C-BAR CFRP bars
	SS3	3 plies of externally bonded CFRP sheets

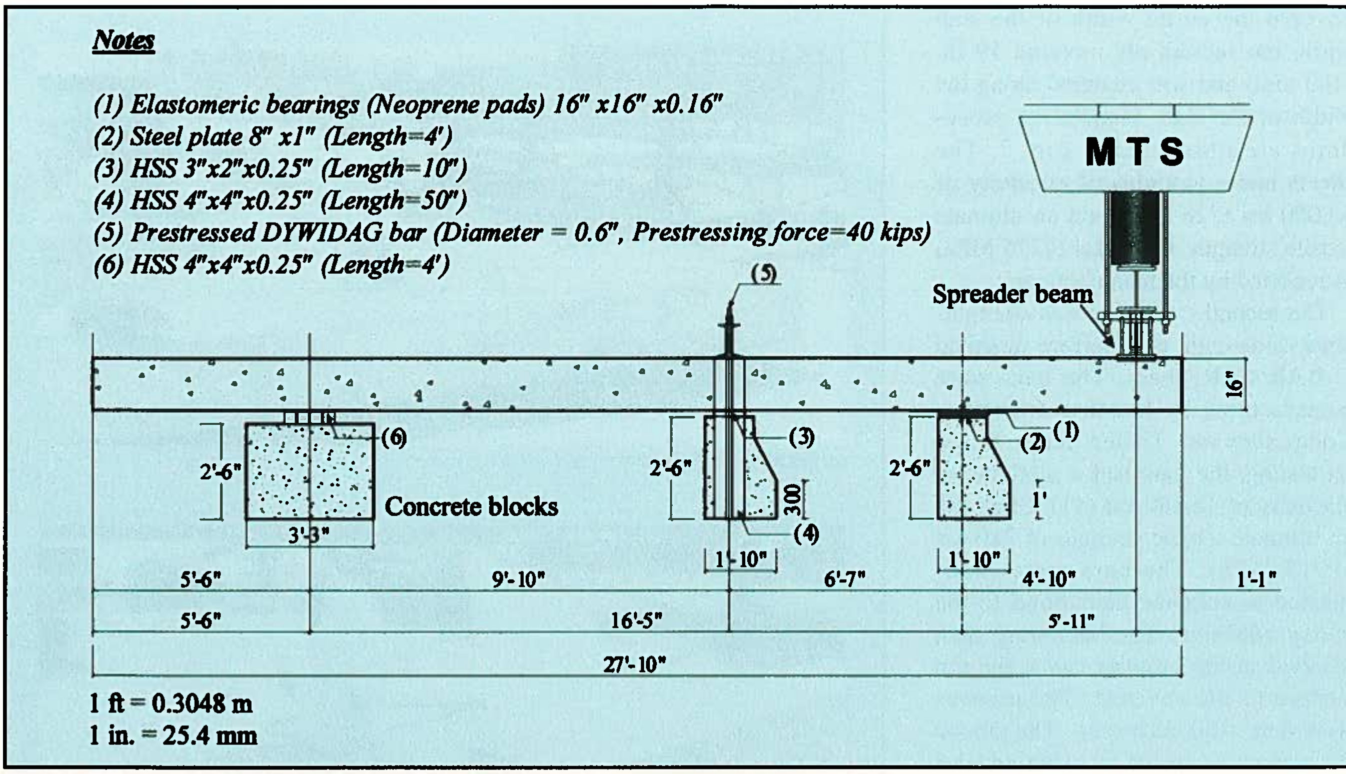

Fig. 8a. Schematic of test setup for cantilever specimens.

Fig. 8b. Testing of cantilever specimens in laboratory.

applied at a distance of 13 in. (330 mm) from the cantilever edge.

To prevent possible damage to the other cantilever during the first test, an intermediate support was provided as shown in Fig. 8a. The test setup for the cantilever tests is shown in Fig. 8b. For the midspan tests, the slab was simply supported with a span of 16 ft (4.90 m), and the load was applied at the center of the slab as shown in Figs. 9a and 9b.

TEST RESULTS AND DISCUSION

This section presents the test results of both cantilever and simply supported tests. The general behavior of each specimen is summarized in the following subsections.

Cantilever Tests

The load-deflection behavior of cantilever specimens strengthened with near surface mounted Leadline bars (C2), CFRP strips (C4), and C-Bars (C6) is compared to the unstrengthened Specimen (C1) as shown in Fig. 10. Test results indicate identical behavior for all the specimens until cracking occurred at a load level of 40.5 kips (180 kN) for the unstrengthened cantilever and 42.7 kips (190 kN) for the strengthened cantilevers.

After cracking, a nonlinear behavior was observed up to failure. The measured stiffnesses for the strengthened specimens were higher due to the addition of the CFRP reinforcement.

The presence of CFRP reinforcement precluded the flattening of the load-deflection curve, which was clear in the control specimen at the load range of 99 to 105 kips (440 and 466 kN). Prior to yielding of the steel reinforcement at a load level of 99 kips (440 kN), the stiffnesses of all strengthened cantilevers were almost the same and were 1.5 times higher than the stiffness of the unstrengthened cantilever.

The presence of the CFRP reinforcement provided constraint to opening of the cracks. Therefore, the deflections were reduced and consequently appeared to increase the stiff-

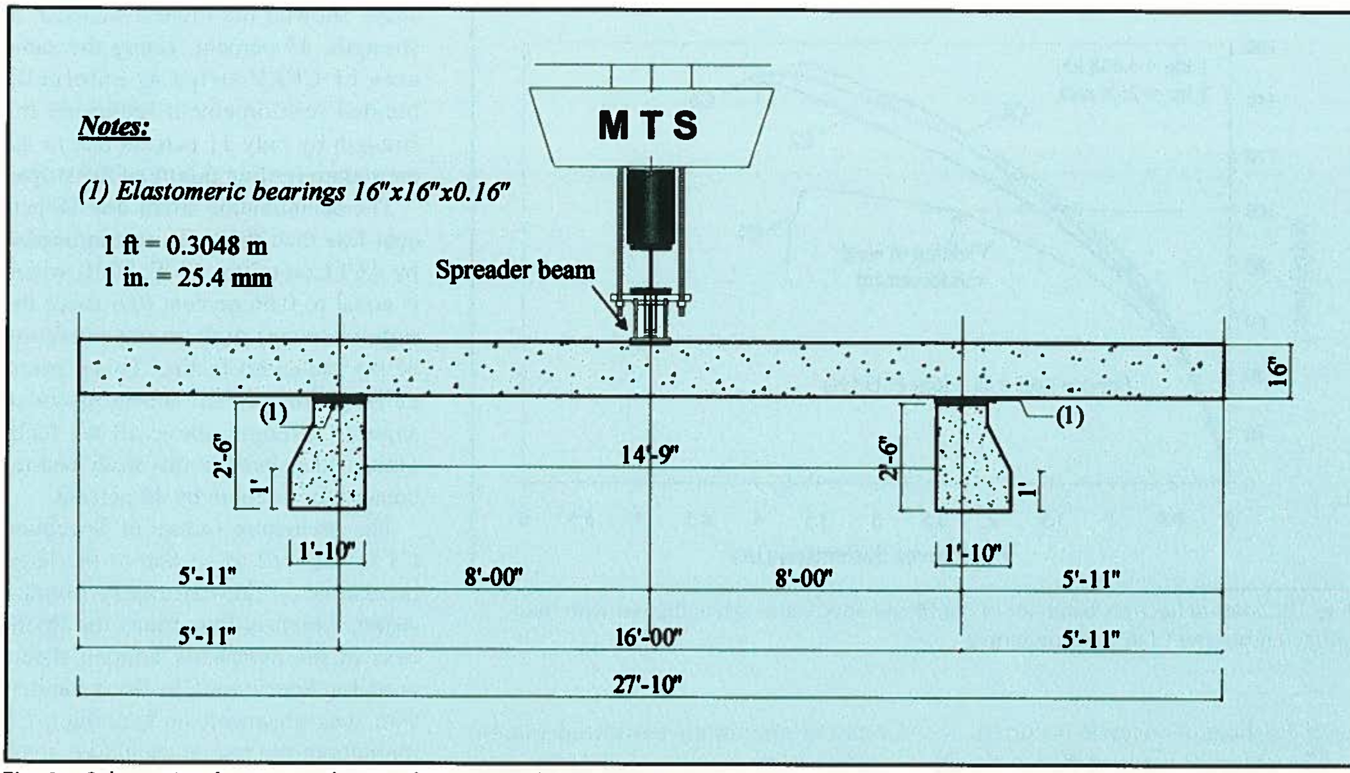

Fig. 9a. Schematic of test setup for simply supported specimens.

ness. After yielding of the tension steel reinforcement, the stiffness of the cantilever specimen strengthened with Leadline bars, Specimen C2, was three times higher than that of the unstrengthened one.

Using C-BAR CFRP bars instead of Leadline bars increased the stiffness by an extra 20 percent. However, using near surface mounted CFRP strips yielded a stiffness increase of 35 percent compared to the Leadline bars. For the control specimen, the increase in the applied load was negligible after yielding of the steel reinforcement. For strengthened cantilevers, the load resistance and deflection increased until the concrete crushed in the compression zone. This is due to additional strength and stiffness provided by the CFRP reinforcement.

Fig. 11 shows the load-deflection behavior of cantilever specimens, C3 and C5, strengthened with externally bonded CFRP strips and sheets, respectively. The behavior of the control specimen, C1, is also shown for comparison. The figure clearly indicates that the strength, stiffness, and ductility were significantly improved with the addition of CFRP reinforcement. Identical behavior was observed for


Fig. 9b. Testing of simply supported specimens in laboratory.

Specimens C3 and C5 up to a load level of 112 kips (500 kN).

After yielding of the steel reinforcement, the stiffness of Specimen C5 was about 3.3 times higher than that of the unstrengthened cantilever. Loading of the cantilever specimens was paused every 11 kips (50 kN) to manually record the strain in demec points attached to the concrete surface. This was reflected by the continuous rise and fall in the load-deflection curves shown in Figs. 10 and 11.

Initial cracking in the concrete substrate at the anchorage zone was observed at a load level of 90 kips (400 kN) for Specimen C3, as shown in Fig. 12. Upon additional loading, the cracks continued to widen up to a load level of 119 kips (530 kN), where unstable delamination occurred resulting in peeling of the strips. The load dropped to a level corresponding to the yield strength of the cross section

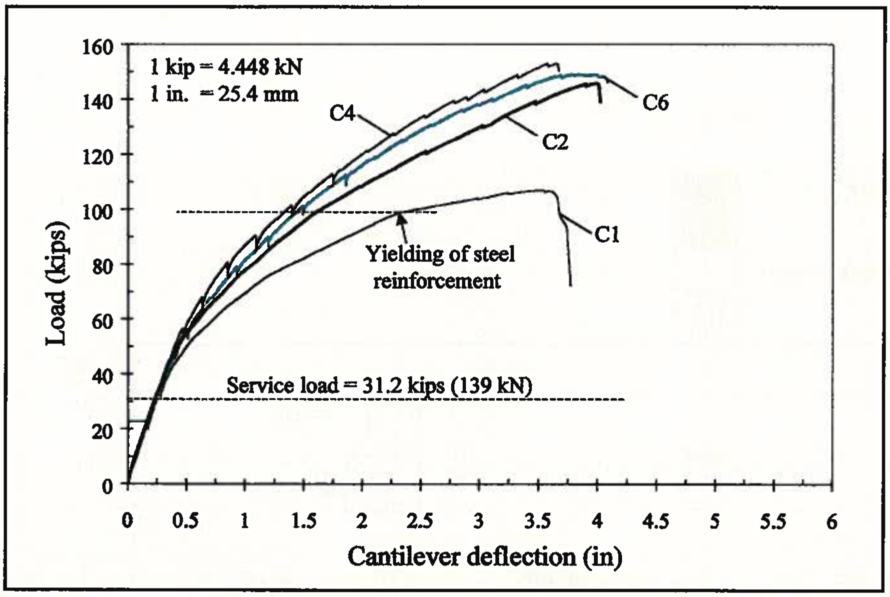

Fig. 10. Load-deflection behavior of cantilever specimens strengthened with near surface mounted CFRP reinforcement.

until crushing of concrete occurred.

The observed mode of failure for all other cantilever specimens was due to crushing of the concrete in the compression zone at the face of the support. At the onset of failure, the bottom steel bars and the steel stirrups were exposed, followed by buckling of the bottom steel bars. Experimental results for the cantilever specimens are summarized in Table 2.

In general, the CFRP-strengthened cantilever specimens showed considerable enhancement of strength. The control specimen exhibited plastic failure with concrete failing in compression and steel yielding.

The failure load of the control specimen was 107 kips (476 kN). Strengthening the specimen using near surface mounted Leadline bars increased the strength by 36 percent in comparison to the design value of 30 percent. Using C-BAR CFRP bars instead of Leadline bars increased the strength by 39 percent.

The cantilever specimen strengthened with near surface mounted CFRP strips showed the highest increase in strength, 43 percent. Using the same area of CFRP strips as externally bonded reinforcement increased the strength by only 11 percent due to the premature peeling failure of the strips.

The delamination strain was 18 percent less than the value recommended by ACI Committee 440F, 2001, which is equal to 0.66 percent (0.5 times the rupture strain) without consideration of the reduction factor.[8] Using externally bonded CFRP sheets provided superior strength above all the techniques considered in this study and increased the strength by 44 percent.

The premature failure of Specimen C3 is believed to be due to the large thickness of the externally bonded strips, which is four times the thickness of the externally bonded sheets used for Specimen C5. No delamination was observed in Specimen C5 throughout the test. It should be noted that near surface mounted strips have double the bond area compared to externally bonded strips.

Typical failure due to crushing of concrete is shown in Fig. 13. The applied load versus crack width relationships for the cantilever specimens strengthened with near surface mounted CFRP strips, C4, and externally bonded CFRP sheets, C5, are shown in Fig. 14, compared to the control specimen. In general, these two techniques have proved their superior efficiency and decreased the crack width by 50 to 70 percent compared to the control specimen.

The Japan Society of Civil Engineers, 1997,[9] The Canadian Highways Bridge Design Code, 1996,[10] and ACI Committee 440F, 2001,[8] set the maximum allowable crack width to 0.020 in. (0.5 mm) for exterior exposure when FRP reinforcement is used. Using a maximum allowable crack width of 0.02 in. (0.5 mm), Fig. 14 shows that Specimens C4 and C5 can sustain a service load level of 92 kips (410 kN), which is three times the AASHTO HSS30 truck design load.

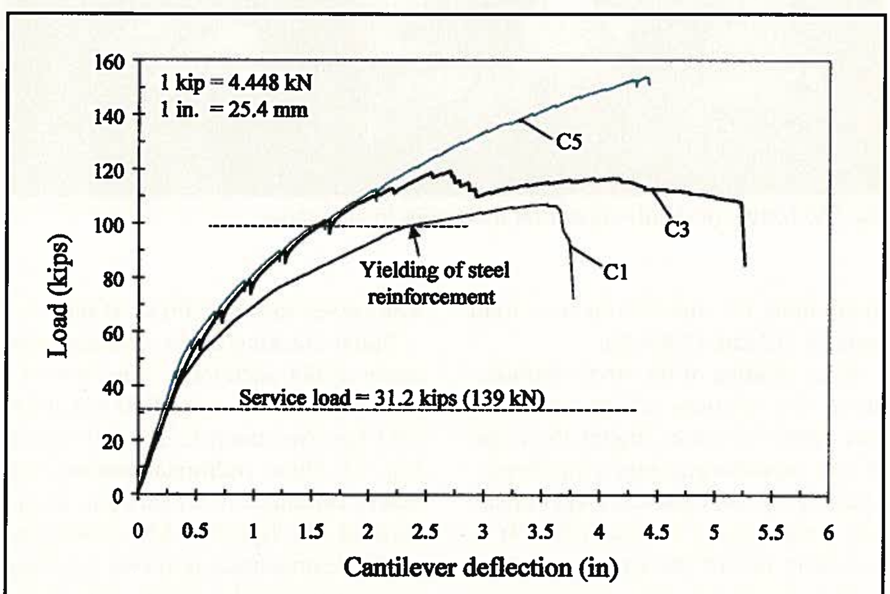

Fig. 11. Load-deflection behavior of cantilever specimens strengthened with externally bonded CFRP reinforcement.

Simply Supported Tests

The load-deflection behavior of the simply supported specimens strengthened with CFRP reinforcement is

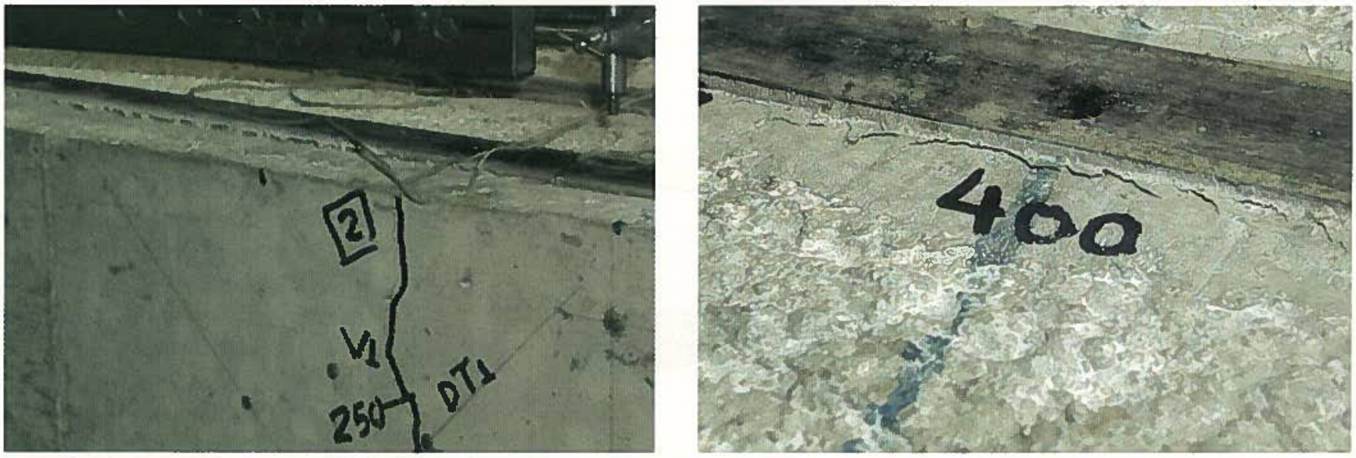

Fig. 12. Initial cracking in concrete substrate of Specimen C3 at 90 kips (400 kN).

shown in Fig. 15. To investigate different strengthening techniques, it was decided not to test a control specimen for the midspan and to rely on the results obtained from nonlinear finite element analysis.[11]

The finite element model was carefully calibrated to the behavior of the unstrengthened cantilever specimen. Strengthening of the specimens slightly increased the cracking load. However, this behavior is also influenced by the value of the tensile strength used in the analysis in comparison to the actual values.

Results indicated a considerable increase in stiffnesses and ultimate loads with the addition of the CFRP reinforcement. Fig. 15 shows that the CFRP reinforcement did not contribute very much to an increase in stiffness in the elastic range of the slabs. However, the stiffnesses of the strengthened slabs were significantly enhanced in the post-cracking region compared to the unstrengthened specimen. Identical behavior was observed for all specimens until cracking occurred at a load level of 78 kips (348 kN) for the unstrengthened slab and 81 kips (360 kN) for strengthened slabs.

The midspan deflection curves showed traditional nonlinearities due to cracking of the concrete and yielding of the steel. Prior to yielding of the bottom tension steel reinforcement, the stiffnesses of all strengthened slabs were almost the same and were 1.5 times higher than the stiffness of the unstrengthened slab. Specimens SS1 and SS2, strengthened with near surface mounted Leadline bars and near surface mounted CFRP strips, re-

Table 2. Experimental results of cantilever specimens.

Specimen	Strengthening technique	P_{cr} (kips)	Δ_{cr} (in.)	P_u (kips)	Δ_u (in.)	Percent increase in capacity
C1	N.A. (Control)	40.5	0.36	107	3.64	—
C2	Near surface mounted Leadline bars	42.5	0.33	145.5	4.02	36
C3	Externally bonded CFRP strips	43.2	0.36	119*	1.54	11
C4	Near surface mounted CFRP strips	42.0	0.33	153	3.66	43
C5	Externally bonded CFRP sheets	43.6	0.36	154	4.41	44
C6	Near surface mounted C-BAR	44.3	0.33	149	3.94	39

Note: 1 kip = 4.448 kN; 1 in. = 25.4 mm.
* Specimen C3 failed due to delamination of CFRP strips, followed by crushing of concrete.
P_{cr} = cracking load
P_u = ultimate load
Δ_{cr} = deflection at cracking
Δ_u = deflection at failure

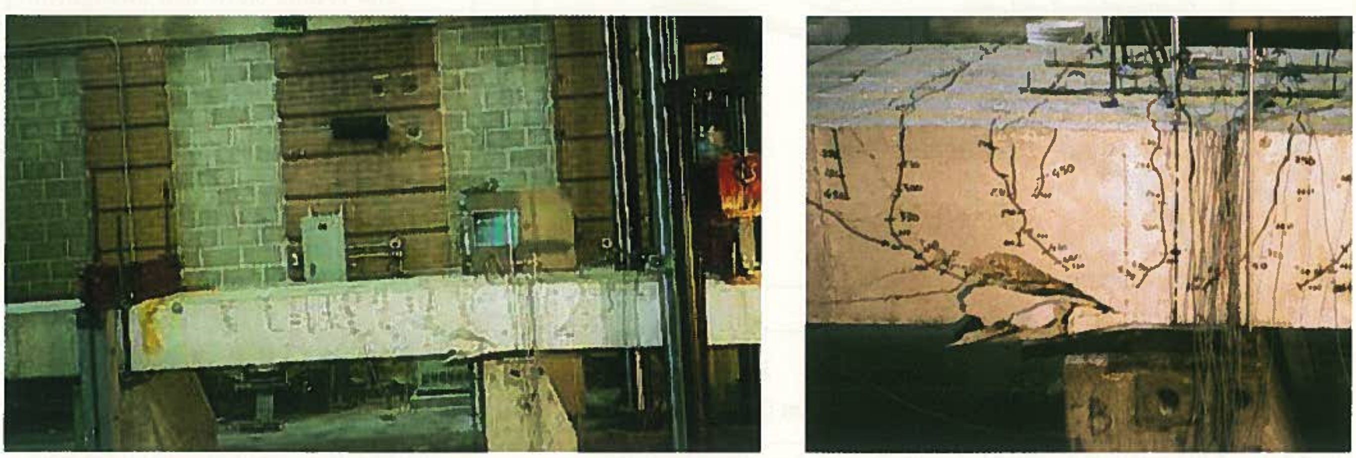

Fig. 13. Overview and closeup of typical failure due to crushing of concrete for cantilever specimens.

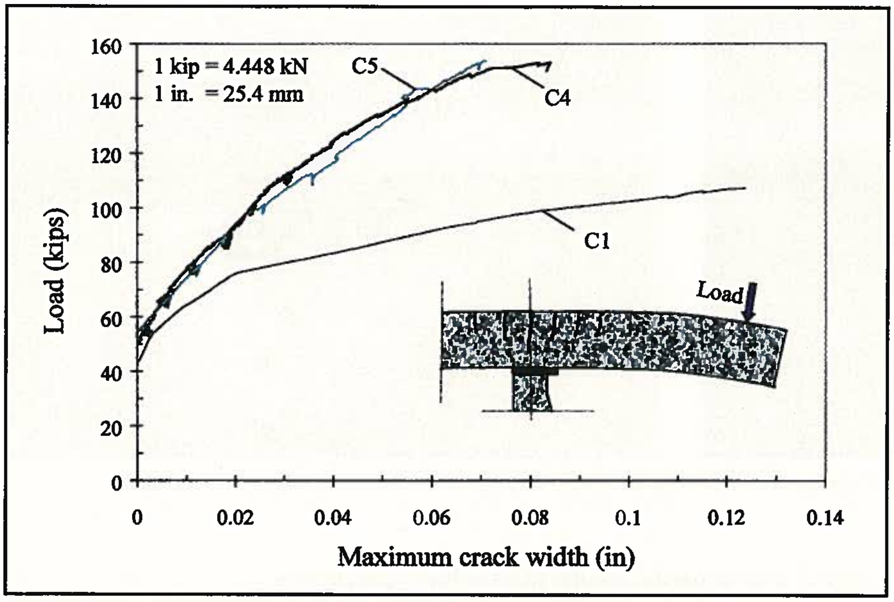

Fig. 14. Load versus crack width for cantilever specimens.

spectively, showed comparable stiffnesses up to failure.

After yielding of the tension steel reinforcement at a load level of 148 kips (660 kN), the stiffnesses of Specimens SS1 and SS2 were three times higher than that of the unstrengthened slab. Using externally bonded CFRP sheets in Specimen SS3 increased the stiffness by an extra 25 percent.

Traditional flexural failure due to crushing of the concrete at the midspan section was observed for all three specimens. Typical crack pattern development for the strengthened simply supported specimens is shown in Fig. 16. The unstrengthened slab exhibited classical failure due to crushing of the concrete at a load level of 167 kips (741 kN). Experimental results of simply supported specimens are given in Table 3.

Strengthening the slab using near surface mounted Leadline bars increased the strength by 34 percent in comparison to the design value of 30 percent. Using near surface mounted CFRP strips instead of Leadline bars increased the strength by 38 percent. Using externally bonded CFRP sheets provided the highest increase in strength by 50 percent.

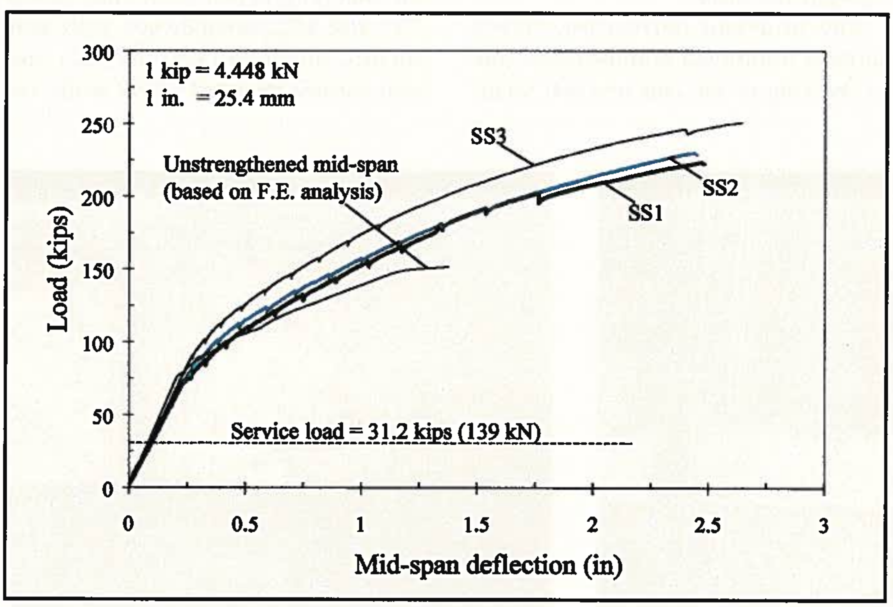

Fig. 15. Load-deflection behavior of simply supported specimens.

COST ANALYSIS

One of the prime objectives of this investigation was to provide a cost-effective analysis for each strengthening technique considered in this study. It should be mentioned that all techniques were designed to increase the strength by 30 percent using the characteristics of each FRP material. An approximate cost for each strengthening technique used for the cantilever specimens is given in Table 4. The total construction cost accounts for the cost of materials, equipment, and labor.

The percentage increase in the flexural capacity and the construction cost for each of the strengthening techniques considered in this study for the cantilever specimens are shown in Fig. 17a. The figure indicates that using near surface mounted CFRP strips and externally bonded CFRP sheets provided the maximum increase in strength. The construction cost of externally bonded CFRP sheets was only 25 percent in comparison to near surface mounted strips. Using either near surface mounted Leadline bars or C-BAR CFRP bars provided approximately the same increase in ultimate load carrying capacity.

With respect to cost, strengthening using C-BAR CFRP bars was 50 percent less. Using an efficiency scale (E) defined by Eq. (1), the efficiency of each technique was evaluated as shown in Fig. 17b:

$$E = \frac{\text{Percent increase in strength}}{\text{Construction cost in USD}} \times 100 \qquad (1)$$

The results show that strengthening using externally bonded CFRP sheets is the most efficient technique in terms of strength improvement and construction cost. The estimated cost of the rehabilitative work for the bridge under consideration was approximately $1 million (USD), which was 60 percent of the cost of demolition and replacement of the existing structure.

ANALYTICAL MODELING

This section summarizes the nonlinear finite element analysis, conducted to simulate the behavior of the post-tensioned bridge slabs strengthened with FRP. The analytical prediction is compared to the experimental results. Up-to-date but very limited information has been reported on the use of nonlinear finite element techniques to simulate the overall behavior of prestressed concrete members strengthened with FRP. Some analyses are reported on the normal and shear stress distributions at the end zones of the FRP strip/sheet.

The finite element modeling described in this paper was conducted using the program ANACAP (Version 2.1). ANACAP is known for its advanced nonlinear capabilities of the concrete material model.[12] The ANACAP software employs the classical incremental theory of plasticity that relates the increment of plastic strain to the state of stresses and stress increment.

Formulation of the yield surfaces, loading, and failure surfaces take into account the effect of confinement on the concrete behavior. The concrete material is modeled by the smeared cracking methodology in which progressive cracking is assumed to be distributed over an entire element.[13] Over the past 35 years, the distributed smeared crack model has been used for plane stress, plane strain and three-dimensional solid systems.[14, 15]

Cracks are assumed to form perpendicular to the principal tensile strain direction in which the cracking criterion is exceeded. When cracking occurs, the stress normal to the crack direction is reduced to zero, which results in redistribution of stresses around the crack. The ability of cracked concrete to share the tensile forces with the steel/FRP reinforcement between cracks is modeled in ANACAP by means of the tension softening model. The descending branch of the tensile stress-strain curve is assumed to follow an exponential function. Cracks are allowed to form in the three principal directions.

The program also accounts for the reduction in shear stiffness due to cracking and further decay as the crack opens.[12] The reinforcement is assumed to be distributed throughout the concrete element. Full bond is assumed between the reinforcement and concrete.

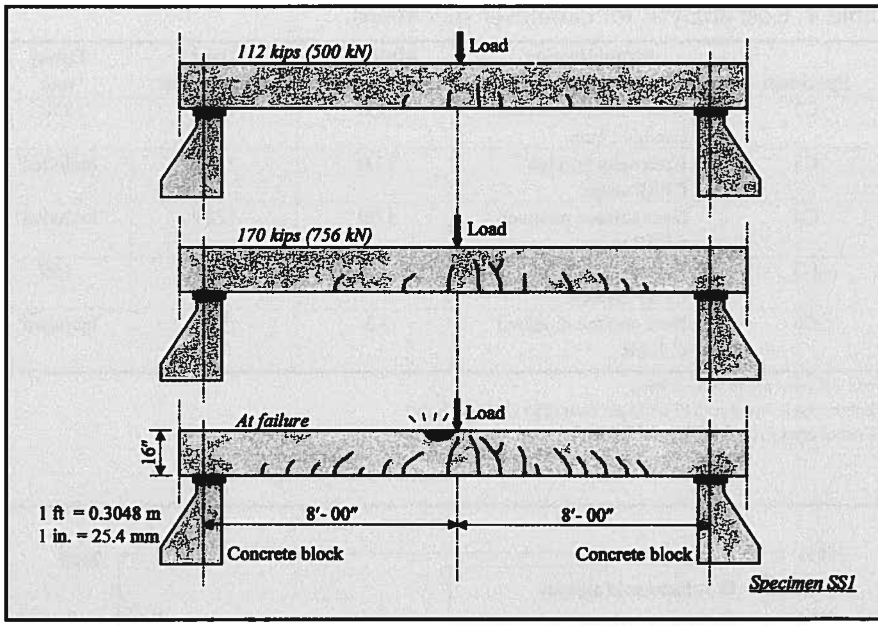

Fig. 16. Typical crack pattern development for strengthened simply supported specimens.

Interfacial failures are not considered in ANACAP. Consequently, peeling failures cannot be predicted and the analysis will be limited to failures due to crushing of the concrete or rupture of the FRP reinforcement. The analysis is conducted using an incremental-iterative solution procedure, in which the load is incrementally increased. Within each increment, equilibrium is iteratively achieved.

Iteration is repeated until internal equilibrium conditions are sufficiently fulfilled and convergence is obtained. At the end of each step, the ANACAP program adjusts the stiffness matrix to reflect the nonlinear changes in the stiffness. Verification of the ANACAP program using independent experimental results can be found elsewhere.[16, 17]

Modeling of the Cantilever Slab

The cantilever slab and adjacent panel were modeled to account for the continuity effect. Taking advantage of the symmetry of the cantilever slab, only one-half of the slab in the longitudinal direction was modeled. The concrete was modeled using 20-node isoparametric brick elements with a 2 x 2 x 2 reduced Gauss integration scheme. Each node has three translational degrees of freedom. The slab was supported on elastic springs having the same stiffness of the neoprene pads used in the test program.

The load was applied as a uniform pressure acting on an area of 9 x 24 in. (228 x 610 mm). The load was applied gradually using a step-by-step analysis. The number of load steps and step size were chosen based on the experience gained through different analytical simulations conducted on bridge deck slabs. The influence of the step size at failure is performed and reported elsewhere.[18]

Three analytical simulations were carried out by varying the size of the elements at the anticipated failure zone and the number of layers within the slab thickness. The number of ele-

Table 3. Experimental results of simply supported specimens.

Specimen	Strengthening technique	P_{cr} (kips)	Δ_{cr} (in.)	P_u (kips)	Δ_u (in.)	Percent increase in capacity*
SS1	Near surface mounted Leadline bars	79	0.26	223	2.5	34
SS2	Near surface mounted CFRP strips	83	0.26	230	2.4	38
SS3	Externally bonded CFRP sheets	81	0.27	251	2.6	50

Note: 1 kip = 4.448 kN; 1 in. = 25.4 mm.
* Ultimate load of unstrengthened specimen was based on nonlinear finite element analysis.

Table 4. Cost analysis for cantilever specimens.

Specimen	Strengthening technique	Material cost per ft	Total material cost	Epoxy cost	Labor hours*	Equipment cost	Total cost
C2	Near surface mounted Leadline bars	12.6	1058	150	7	67	1394
C3	Externally bonded CFRP strips	17.0	1224	Included†	5	None	1309
C4	Near surface mounted CFRP strips	17.0	1224	Included†	9	67	1444
C5	Externally bonded CFRP sheets	7.0	252	150	4	34	354
C6	Near surface mounted C-BAR	3.5	336	Included†	9	100	739

Note: All costs are in U.S. dollars.

* Labor cost is based on $17 USD per hour ($25 CAD per hour).

† Cost of epoxy is included in the material's cost.

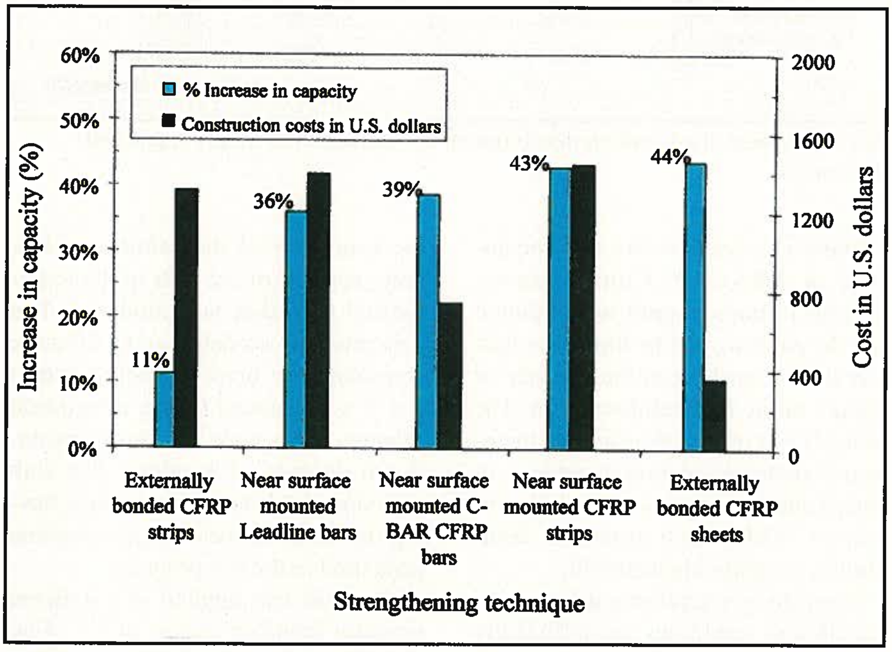

Fig. 17a. Cost analysis of various strengthening techniques.

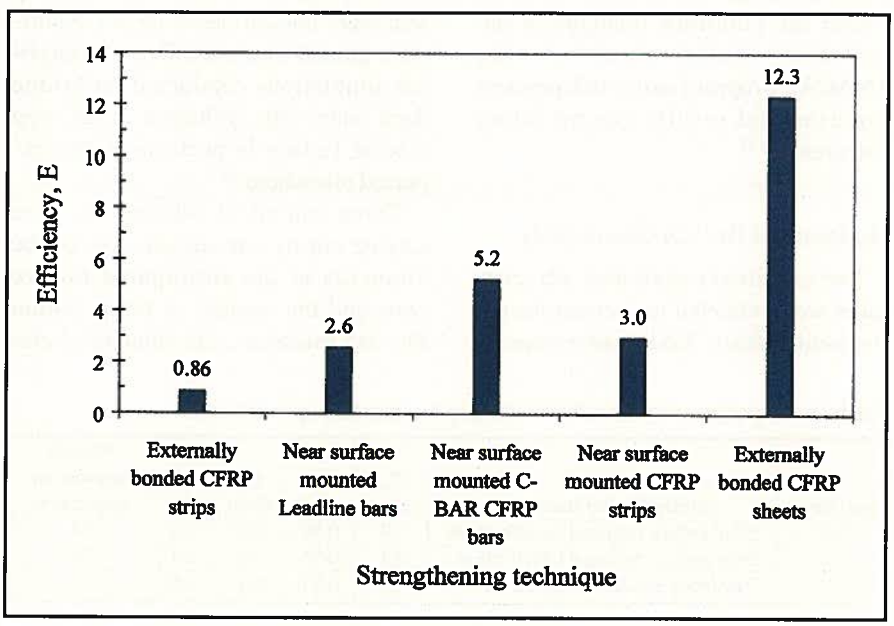

Fig. 17b. Efficiency of various strengthening techniques.

ments varied from 324 elements in the first mesh to 924 elements in the third mesh for the unstrengthened specimen. Mesh dimensions for the three cases are shown in Fig. 18. The variation in element size was employed to provide a fine mesh around the area of maximum bending and shear stresses.

The predicted load-deflection behavior of the three numerical simulations is shown in Fig. 19, where the results are compared to the measured values for the unstrengthened specimen, C1. The response was relatively brittle when small size elements were used. Deformation at failure increased with the increase of the element size.

As expected, the deformational behavior was quite similar for the various simulations. The influence of the mesh size on the predicted failure loads was noticeable. The predicted failure load was 97 kips (430 kN) when coarse mesh was used. Refining the finite element mesh resulted in a considerable increase in the predicted failure loads.

Compared to the test results, it emerged for the second mesh that the flexural stiffness was predicted with sufficient accuracy up to failure. From the above discussion, it is concluded that using the second mesh in modeling cantilever specimens revealed sufficient accuracy. It should be mentioned that the corresponding execution time was 50 percent less than that of the third mesh.

Modeling of the Simply Supported Slab

Taking advantage of the symmetry of the simply supported specimen,

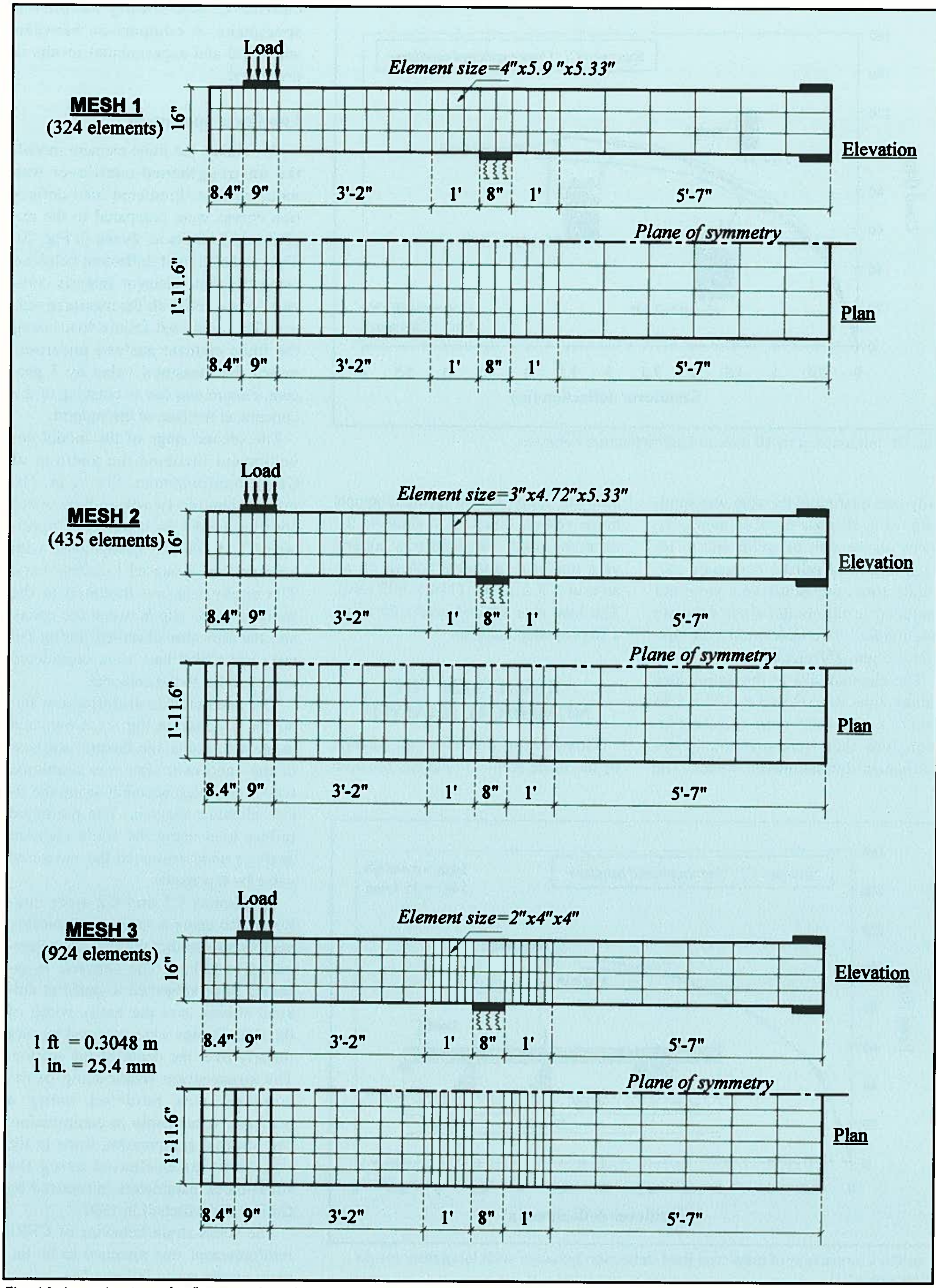

Fig. 18. Investigation of influence of mesh size.

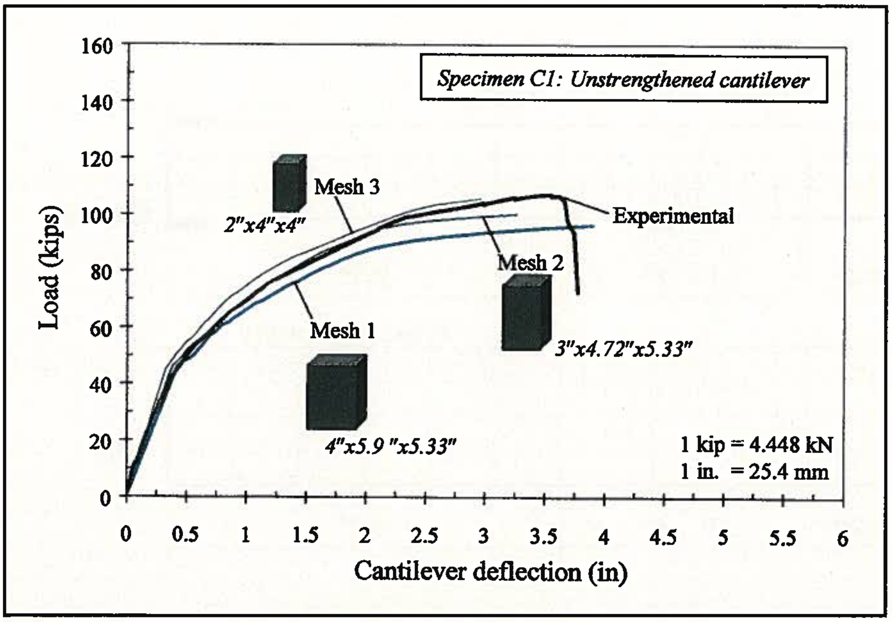

Fig. 19. Influence of mesh size on load-deflection behavior.

only one-quarter of the slab was modeled using 20-node brick elements. To focus on the slab behavior and to remain within a realistic computer execution time, the cantilevers were not included in the model since they are not loaded. The specimen was discretized into 255 elements.

The element size at the anticipated failure zone was set to 3 x 4.72 x 5.33 in. (76 x 120 x 135 mm), the same dimensions that were previously described in the cantilever model. The slab was supported on spring elements in the vertical direction to simulate the neoprene pads. The load was applied as a uniform pressure acting on an area of 4.5 x 24 in. (114 x 609 mm). The load was applied gradually using a step-by-step analysis.

RESULTS OF THE NUMERICAL ANALYSIS

This section discusses the results of the finite element analysis for both cantilever and simply supported specimens. A comparison between analytical and experimental results is presented.

Cantilever Specimens

To validate the finite element model, the unstrengthened cantilever was modeled first. Predicted load-deflection curves were compared to the experimental results as shown in Fig. 20. The predicted load-deflection behavior using the finite element analysis compared very well with the measured values. The predicted failure load using the finite element analysis underestimated the measured value by 7 percent. Failure was due to crushing of the concrete at the face of the support.

The second stage of the model development involved the addition of CFRP reinforcement. Six $^3/_8$ in. (10 mm) diameter Leadline bars were added to model the behavior of Specimen C2, which was strengthened with near surface mounted Leadline bars. The epoxy was not modeled in the analysis as no slip between the epoxy and the bars was observed during the test. The CFRP bars were considered to be bonded to the concrete.

The predicted load-deflection behavior is shown in Fig. 21. Compared to the test results, the flexural stiffness of the cantilever slab was simulated with a very high accuracy using the finite element analysis. The predicted failure load using the finite element analysis underestimated the measured value by 6 percent.

Specimens C1 and C2 were analyzed also using a strain compatibility approach to predict the flexural behavior up to failure. The concrete is assumed to be subjected to uniform uniaxial strains over the entire width of the slab. Strains were assumed to vary linearly over the depth of the section. The stress-strain relationship of the concrete was modeled using a parabolic relationship in compression. The internal compression force in the concrete was evaluated using the stress-block parameters introduced by Collins and Mitchell in 1991.[19]

The stress-strain behavior of CFRP reinforcement was assumed to be linearly elastic up to failure. The deflec-

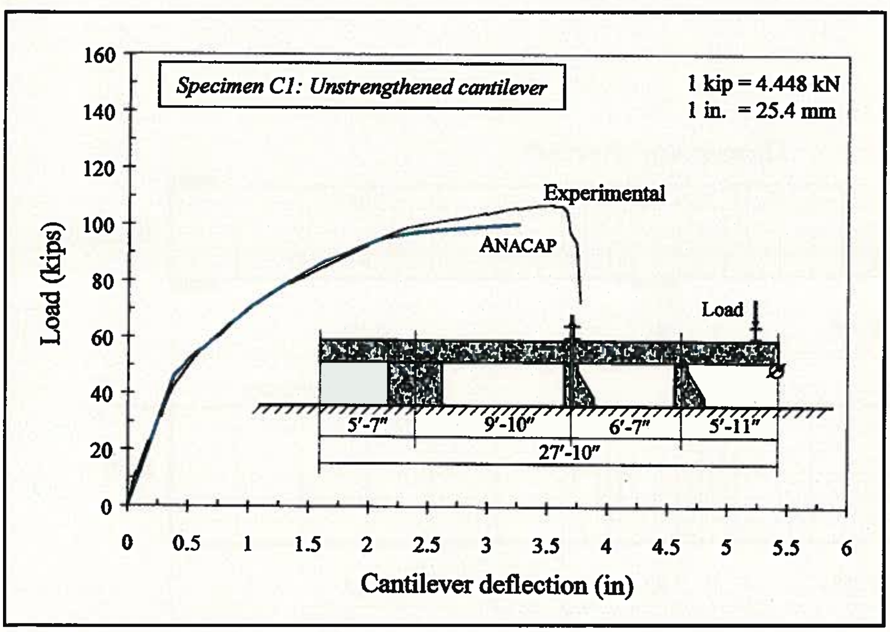

Fig. 20. Comparison of predicted load-deflection behavior with laboratory results (Specimen C1).

tion was calculated by integrating the curvature at each load increment. Predicted loads and deflections at cracking and at failure are given in Table 5.

The predicted failure loads using strain compatibility approach underestimated the measured values for Specimens C1 and C2 by 6 and 10 percent, respectively. Predicting the deflection values using strain compatibility approach underestimated also the initial stiffness of the slabs by 13 percent as given in Table 5.

Simply Supported Specimens

The predicted load-deflection behavior of Specimen SS1, strengthened with near surface mounted Leadline bars is shown in Fig. 22, compared to the measured values. Even though the predicted behavior was very satisfactory, the predicted initial stiffness was overestimated by 11 percent. Such a phenomenon is a direct consequence of previous bending tests conducted on the two cantilevers.

In general, the predicted behavior was in a good agreement in terms of cracking load, ultimate load and flexural stiffness after cracking of the concrete. Failure was due to crushing of the concrete at the location of the applied load. The analysis predicted a failure load of 204 kips (907 kN), which was 9 percent less than the measured value. Compared to the experimental results, the overall behavior was well simulated using the ANACAP program.

CONCLUSIONS

Based on the findings of this investigation, the following conclusions can be drawn:

1. The use of near surface mounted CFRP reinforcement is feasible and cost effective for strengthening or repairing prestressed concrete girders and slabs.

2. Both the stiffness and strength of concrete slabs strengthened with CFRP materials were substantially increased. The ultimate load carrying capacity of the slabs can be increased by as much as 50 percent.

3. The magnitude of strength increase was influenced by the type and

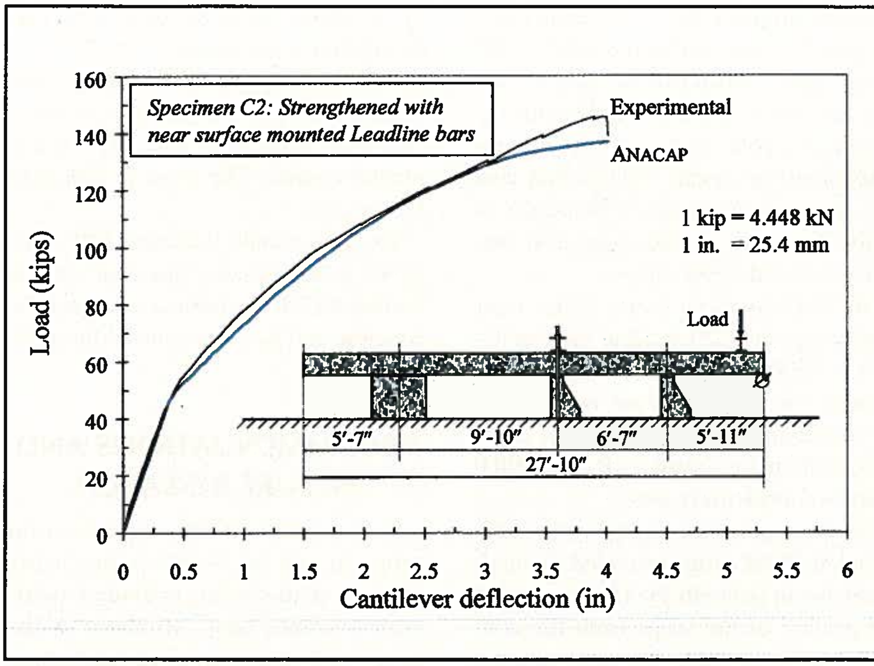

Fig. 21. Comparison of predicted load-deflection behavior with laboratory results (Specimen C2).

Table 5. Predicted results for Specimens C1 and C2.

Specimen	Method of analysis	P_{cr} (kips)	Δ_{cr} (in.)	P_u (kips)	Δ_u (in.)	P_u predicted / P_u experimental
C1	Experimental	40.5	0.36	107	3.64	—
	Finite element	45.0	0.37	100	3.3	0.93
	Strain compatibility	46	0.47	101	2.0	0.94
C2	Experimental	42.5	0.33	145.5	4.02	—
	Finite element	46	0.39	137	4.0	0.94
	Strain compatibility	47	0.42	131	2.7	0.90

Note: 1 kip = 4.448 kN; 1 in. = 25.4 mm.

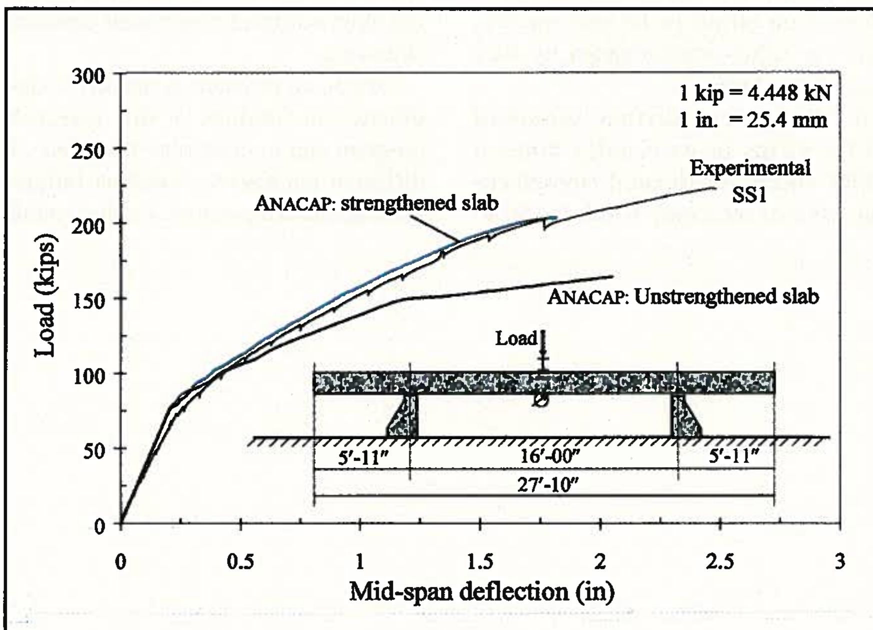

Fig. 22. Comparison of predicted load-deflection behavior with laboratory results (Specimen SS1).

configuration of the CFRP materials. In general, near surface mounted CFRP strips and externally bonded CFRP sheets provided superior strength increase for both cantilever and simply supported specimens. The overall cost of strengthening using CFRP sheets is only 25 percent of that using near surface mounted CFRP strips.

4. Strengthening using either near surface mounted Leadline bars or C-BAR CFRP bars provided approximately the same increase in strength. With respect to construction cost, strengthening using C-BAR CFRP bars is considerably less.

5. Strengthening using externally bonded CFRP strips provided the least increase in strength by 11 percent due to peeling of the strips from the concrete surface. Using the same amount of strips but as near surface mounted reinforcement enhanced the ultimate load carrying capacity by 43 percent. Groove dimensions of 0.2 in. wide by 1 in. deep (5 x 25 mm) were adequate to prevent splitting of the epoxy cover.

6. Strengthening using externally bonded CFRP sheets is the most efficient technique in terms of strength improvement and construction cost.

7. Delamination of the CFRP strips occurred at a strain of 0.54 percent, which is equivalent to 41 percent of the rupture strain of the strips as reported by the manufacturer. The delamination strain is 18 percent less than the value recommended by ACI Committee 440F.

8. Using near surface mounted CFRP strips or externally bonded CFRP sheets for flexural strengthening reduced the crack width by 50 to 70 percent compared to the unstrengthened specimen.

9. The predicted results using nonlinear finite element analysis were in excellent agreement with the experimental results. The error is less than 10 percent.

10. Test results indicated full composite action between the near surface mounted CFRP reinforcement and the concrete and no slip occurred throughout the tests.

RECOMMENDATIONS AND FUTURE RESEARCH

Test results of the experimental program and predicted values using numerical modeling provided sufficient evidence and confidence of the proposed strengthening technique using near surface mounting as a new and promising technology. Delamination-type failures, occasionally observed by using externally bonded reinforcement, can be precluded using this technique.

Epoxy adhesives commonly used for bonding steel bars have proved to be effective in bonding CFRP bars. However, characterizing the bond performance of the adhesives is compulsory prior to any application. It is recommended to use the groove dimensions outlined in this paper for near surface mounted bars and strips for strengthening reinforced and prestressed concrete structures.

Additional research is needed to duplicate the findings of this research program and to determine the effect of different parameters, such as fatigue loading and temperature, on the overall behavior. Analytical models describing the load transfer mechanism of near surface mounted FRP reinforcement to concrete are urgently needed.

Work is currently under way by the authors to provide complete design guidelines regarding the development length needed for the proposed FRP strengthening techniques; these will be reported in a future paper. The authors recommend also that future research be focused on examining the durability aspects of various FRP strengthening systems under severe environmental conditions.

ACKNOWLEDGMENTS

The authors wish to acknowledge the support of the Network of Centres of Excellence, ISIS Canada, program of the Government of Canada and the Natural Science and Engineering Research Council. The writers gratefully acknowledge the support provided by Mitsubishi Chemical Corporation, Japan, Marshall Industries Composites Ltd., United States, S&P Clever Reinforcement Company, Switzerland, and Master Builders Technologies Ltd., United States, for providing the materials used in the test program.

The authors would like also to acknowledge the support provided by Vector Construction Ltd., Winnipeg, Canada, for performing all the strengthening work. Special thanks are owed to M. McVey for his assistance during the fabrication and testing of the specimens. Finally, the authors want to thank the PCI JOURNAL reviewers for their thoughtful and constructive comments.

REFERENCES

1. U.S. Department of Transportation (DOT), Bureau of Transportation Statistics, Transportation Statistics Annual Report, Washington DC, 1997, 286 pp.
2. Tann, D. B., and Delpark, R., "Experimental Investigation of Concrete Beams Reinforced with Narrow Carbon Strips," Proceedings of the International Conference on Structural Faults and Repair, CD-ROM, 1999.
3. Corry, R., and Dolan, C. W., "Strengthening and Repair of a Column Bracket Using Carbon Fibre Reinforced Polymer (CFRP) Fabric," PCI JOURNAL, V. 46, No. 1, January-February 2001, pp. 54-63.
4. Burke, C. R., and Dolan, C. W., "Flexural Design of Prestressed Concrete Beams Using FRP Tendons," PCI JOURNAL, V. 46, No. 2, March-April 2001, pp. 76-87.
5. AASHTO, *Standard Specifications for Highway Bridges*, American Association for State Highway and Transportation Officials, Washington, DC, 1998.
6. Integrated Finite Element Analysis and Design of Structures, *SAP2000 Graphic User Interface Manual*, Version 7.0, Computer and Structures Incorporation, Berkeley, CA, 1998.
7. Blaschko, M., and Zilch, K., "Rehabilitation of Concrete Structures with Strips Glued Into Slits," Proceedings of the 12th International Conference on Composite Materials, Paris, France, CD-ROM, 1999.
8. ACI Committee 440F, "Guide for the Design and Construction of Externally Bonded FRP Systems for Strengthening Concrete Structures," Draft Report, American Concrete Institute, Farmington Hills, MI, October 2001, 150 pp.
9. Japan Society of Civil Engineers (JSCE), 1997b, "Recommendations for Design and Construction of Concrete Structures Using Continuous Fiber Reinforcing Materials," Concrete Engineering Series, No. 23, Tokyo, Japan, 1997, 325 pp.
10. Canadian Standards Association, *Canadian Highways Bridge Design Code*, Section 16, Fiber Reinforced Structures, Ottawa, Ontario, 1996, 28 pp.
11. Hassan, T., Horeczy, G., Svecova, D., Rizkalla, S., Shehata, E., and Stewart, D., "Flexural Strengthening of Post-Tensioned Bridge Slab Using FRP," Proceedings of the International Conference on Advanced Composite Materials for Bridges and Structures (ACMBS-III), Ottawa, Ontario, 2000, pp. 291-298.
12. James, R. G., *ANACAP Concrete Analysis Program Theory Manual*, Version 2.1, Anatech Corp., San Diego, CA, 1997.
13. Rashid, Y. R., "Analysis of Prestressed Concrete Pressure Vessels," *Nuclear Engineering Design*, V. 7, No. 4, 1968, pp. 334-344.
14. Scordelis, C. A., "Past, Present and Future Development," Seminar on Finite Element Analysis of Reinforced Concrete Structures, Japan Concrete Institute, V. 1, 1985, pp. 203-212.
15. Gerstle, K. H., "Material Modeling of Reinforced Concrete," IABSE Colloquium on Advanced Mechanics of Reinforced Concrete, Introductory Report, Delft, Netherlands, 1981.
16. Hassan, T., Abdelrahman, A., Tadros, G., and Rizkalla, S., "FRP Reinforcing Bars for Bridge Decks," *Canadian Journal of Civil Engineering*, V. 27, No. 5, 2000, pp. 839-849.
17. Mufti, A., Hassan, T., Memon, A., and Tadros, G., "Analytical Study of Punching Shear Strength of Restrained Concrete Slabs," Proceedings of the Canadian Society of Civil Engineering Annual Conference (CSCE), Victoria, British Columbia, CD-ROM, 2001.
18. Hassan, T., "Behavior of Concrete Bridge Decks Reinforced With FRP," M.Sc. Thesis, University of Manitoba, Canada, 1999, 226 pp.
19. Collins, M., and Mitchell, D., *Prestressed Concrete Structures*, Prentice Hall, Englewood Cliffs, NJ, 1991, 766 pp.